2017

Adaptive, Sparse, and Multi-rate LQR Control of an MVDC Shipboard Power System with Constant Power Loads

Mills, Adam J.; Ashton, Robert W.

Mills, Adam J., and Robert W. Ashton. "Adaptive, sparse, and multi-rate LQR control of an MVDC shipboard power system with constant power loads." Industrial Technology (ICIT), 2017 IEEE International Conference on. IEEE, 2017.
http://hdl.handle.net/10945/60783

Adaptive, Sparse, and Multi-rate LQR Control of an MVDC Shipboard Power System with Constant Power Loads

Lieutenant Commander Adam J. Mills, USN
Department of Electrical and Computer Engineering
Naval Postgraduate School
Monterey, CA, USA
ajmills@nps.edu

Robert W. Ashton, Ph.D
Department of Electrical and Computer Engineering
Naval Postgraduate School
Monterey, CA, USA
ashton@nps.edu

Abstract— **The US Navy is pursuing development of all-electric warships. The future all-electric warship is expected to utilize medium-voltage DC (MVDC) main distribution to supply several load zones. The load zones will convert the MVDC power to lower voltage for use by local loads as well as contain local energy storage for casualty back-up power. A majority, if not totality of loads are expected to exhibit constant-power load (CPL) behavior. Voltage instabilities introduced by CPLs and methods to address the problem in multi-machine MVDC systems are reviewed. This paper presents an LQR based, centralized, control scheme to regulate MVDC distribution bus voltage as well as the low-voltage DC (LVDC) service buses through coordinated use of low-bandwidth MVDC voltage sources and high-bandwidth, low-voltage currents sourced from the local energy storage devices. A sparse-feedback, multi-rate LQR controller (LQR-SM) is designed and implemented in MATLAB software using a hypothetical multi-machine, multi-zone shipboard MVDC electric distribution system with CPLs and energy storage devices. The presented control scheme is able to combine and coordinate all available control inputs to effectively regulate MVDC and LVDC buses in the system while allowing for design flexibility not available through existing control schemes.**

Keywords— MVDC, constant power load (CPL), hybrid energy storage system (HESS), linear quadratic regulator (LQR), adaptive, non-linear, all-electric ships.

I. INTRODUCTION

FUTURE warships are expected to include a wide array of computer systems, sensors, and weapon systems, including energy weapons such as lasers or railguns [1]. To meet the rapidly growing demand for electrical power on board modern warships, the US Navy is considering medium voltage DC (MVDC) distribution systems due to their advantages in size, weight, and cost compared to traditional three-phase low voltage architectures [2]. A wide array of power converters will be utilized in MVDC systems to transfer power from the generating modules to the appropriate voltage and frequency required by each load. When coupled with high bandwidth control schemes, power converters behave like constant power loads (CPL) [3]. The negative non-linear impedance of CPLs reduces system stability.

With such extensive use of power electronics, CPLs are expected to make up the bulk of all system loads. Additionally, the inclusion of high energy combat system loads such as dual-band radars, laser weapons and/or electromagnetic railguns have the consequence of substantial pulse load transients. The combination of CPLs and pulsed loads presents a significant challenge to designing a system that has acceptable small and large signal stability since direct linear methods cannot be employed.

A hybrid energy storage system (HESS) consists of a combination of two or more energy storage devices, often through a power electronic interface. HESS may include batteries, flywheels, capacitors, or other energy storage devices [4][5]. HESS may be used as a controlled current source to improve DC bus regulation where stochastic (pulsed or "peaky") loads or sources are present [6].

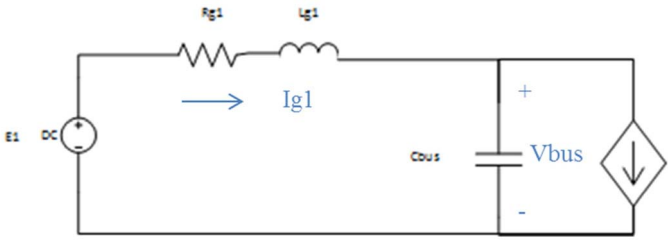

Figure 1 – Second Order Circuit with Constant Power Load

Several recent works have sought to provide stability to systems with CPLs. For the most part, each of the control methods applied to this problem have reduced the system to a 2nd order single-input, single-output control problem in the form of Fig. 1.

Arcidiocono, et al [7] adaptively applied a linear proportional state-feedback controller to a 2nd order circuit, consistent with Fig. 1, in order to achieve the desired dynamic response using the generator voltage as the single control

input. Carmeli, et al [8] addressed the same 2nd order circuit problem, but used a HESS device connected to the MVDC bus to provide the single control input.

Ref. [9] expanded the work further by developing a multi-machine model with voltage sources as the control input. Their approach, however, relied on several simplifying assumptions that would allow a multi-machine circuit model to be reduced to the 2nd order system of Fig. 1. They assumed that cable impedances were negligible and that voltage source series resistance was negligible. This allowed all power sources to be placed in parallel and thus reduced to a single equivalent source. They then applied state-feedback linearization (LSF) to achieve the desired dynamic response. The requirement that power source resistance be ignored was revisited in [10] and replaced with the requirement that the R-L ratios (shown as Rg1 and Lg1 in Fig. 1) of each power source be equal. Again, they reduced a large complex system into a 2nd order system with a single input. Further, [11] applied backstepping control laws in place of state-feedback linearization using the same simplifications as [10] and achieved good results.

The constraint that the R-L ratios of each power source be equal was removed in [12] by the use of linear quadratic Gaussian control. In essence, this technique modeled each power source as a separate system with separate control. The linearized load resistance for each power source sub-system was estimated using an estimating Kalman filter and control provided by a linear quadratic regulator (LQR) controller. This method decentralized control allowing each power source to attempt to control the MVDC bus voltage. This opens the possibility that controllers may counteract one another and provide sub-optimal total system response.

This research presents a sparse-feedback, multi-rate LQR controller (LQR-SM) to regulate the MVDC and LVDC buses in a hypothetical multi-machine MVDC shipboard electric distribution system that includes HESS, CPLs, and pulsed loads. The proposed control method is multi-input, therefore allowing the coordinated use of all available control inputs, such as MVDC power supplies and HESS current sources. This method does not require substantial simplification of complex systems and accommodates the use of control inputs of differing bandwidths.

II. System Model

The hypothetical MVDC shipboard distribution system consists of two power generation modules (PGM), an MVDC main bus, and two load zones. Each of the two load zones is connected to the MVDC main bus by line cabling, an intermediate DC-DC converter input side damper filter, and an intermediate DC-DC converter operating in continuous conduction mode. Within each zone is a HESS and an ideal CPL load.

Each of the PGMs is imagined as a prime mover driving an AC generator. The generator output is rectified and fed to a DC-DC converter. For simulation, we use average value models consisting of a controlled voltage source in series with equivalent resistance and inductance with a parallel capacitor. Each PGM interfaces directly to a 12kV MVDC main bus. Due to the relatively high voltage of the MVDC bus, a reasonable switching frequency of 1kHz is assumed for the PGMs. One PGM will be 40MW while the other will be 10MW for a total of 50MW of generating capacity.

To account for shipboard cabling, equivalent line impedance is modeled in series with each load zone. The values for the bus impedances were derived from [9] for 300 meters of cable. Each load zone consists of a series damped RC filter in parallel with the medium voltage side of a power conversion module (PCM). PCMs are modeled as Buck DC-DC converters operating in continuous conduction mode (CCM) at a fixed duty cycle. The average value model of the DC-DC converter is a controlled current source on the medium voltage side and a controlled voltage source on the low voltage side. The power flow into the converter is held equal to the power flow out of the converter to maintain conservation of power. The equivalent average value Buck inductance and filter capacitance are modeled on the low voltage side of the converter. Since the HESSs act in relatively low voltage compared to the PGMs, they are switched with much greater speed than the PGMs, 8kHz. All loads within the zones are ideal CPLs. The first load zone has a 20MW CPL on a 1kV bus while the second zone has a 30MW CPL on a 6kV bus. An overview block diagram of the distribution system is shown in Fig. 2 with the circuit model shown in Fig. 3.

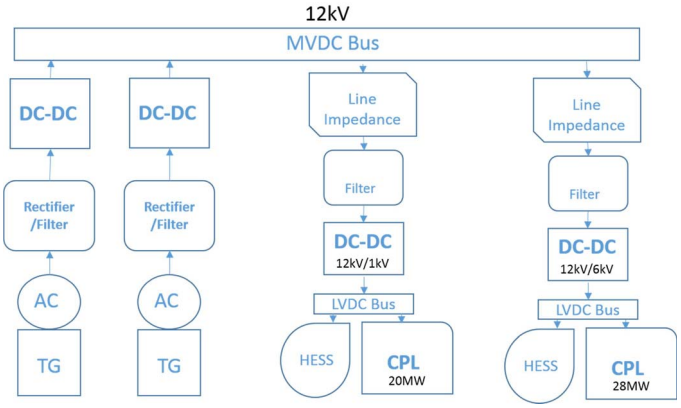

Figure 2 - Simplified Illustration of Shipboard MVDC Distribution System

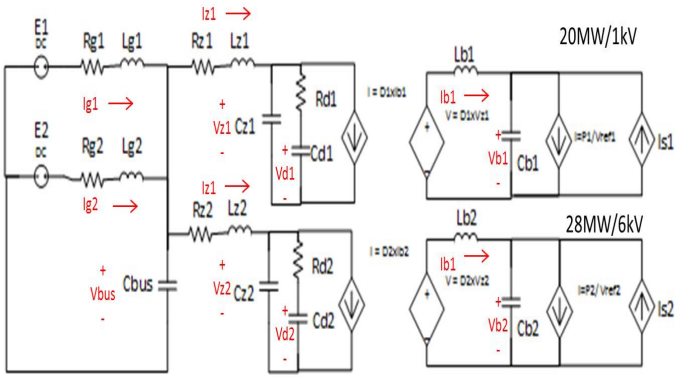

Figure 3 – Average Value Circuit Model of Shipboard MVDC Distribution System

The Fig. 3 circuit model differential equations are shown in (1).

$$
\begin{aligned}
dIg_1 &= \left(\frac{1}{Lg_1}\right) * \left(E_1 - Rg_1 * Ig_1 - V_{bus}\right) \\
dIg_2 &= \left(\frac{1}{Lg_2}\right) * \left(E_2 - Rg_2 * Ig_2 - V_{bus}\right) \\
dV_{bus} &= \left(\frac{1}{C_{bus}}\right) * \left(Ig_1 + Ig_2 + Ig_3 + Ig_4 - Iz_1 - Iz_2 - Iz_3\right) \\
dIz_1 &= \left(\frac{1}{Lz_1}\right) * \left(V_{bus} - Rz_1 * Iz_1 - Vz_1\right) \\
dIz_2 &= \left(\frac{1}{Lz_2}\right) * \left(V_{bus} - Rz_2 * Iz_2 - Vz_2\right) \\
dVz_1 &= \left(\frac{1}{Cz_1}\right) * \left(Iz_1 - Id_1 - d_1 * Ib_1\right) \\
dVz_2 &= \left(\frac{1}{Cz_2}\right) * \left(Iz_2 - Id_2 - d_2 * Ib_2\right) \\
dVd_1 &= \left(\frac{1}{Cd_1}\right) * \frac{Vz_1 - Vd_1}{Rd_1} \\
dVd_2 &= \left(\frac{1}{Cd_2}\right) * \frac{Vz_2 - Vd_2}{Rd_2} \\
dIb_1 &= \left(\frac{1}{Lb_1}\right) * \left(d_1 * Vz_1 - Vb_1\right) \\
dIb_2 &= \left(\frac{1}{Lb_2}\right) * \left(d_2 * Vz_2 - Vb_2\right) \\
dVb_1 &= \left(\frac{1}{Cb_1}\right) * \left(Ib_1 - \frac{P_1}{Vb_1} + Is_1\right) \\
dVb_2 &= \left(\frac{1}{Cb_2}\right) * \left(Ib_2 - \frac{P_2}{Vb_2} + Is_2\right)
\end{aligned}
\tag{1}
$$

where:
E_x is the PGM voltage
Ig_x is the PGM inductor current
V_{bus} is the MVDC bus voltage
Iz_x is the line current to zone 'x'
Vz_x is the voltage at the input to Buck converter 'x'
Vd_x is the voltage across the damper capacitor for zone 'x'
Ib_x is the Buck inductor current for zone 'x'
Vb_x is the voltage on the Buck filter capacitor for zone 'x'
Is_x is the current injected from HESS 'x'
d_x is the duty cycle for the Buck converter for zone 'x'

The circuit topology does not lend itself to simplification to a 2nd order model as described in Refs. [7]-[12]. The CPLs in Fig. 3 are separated from the main bus by intermediate DC-DC converters. The load zones are not simplified into CPLs since the intermediate DC-DC converters are also operating at 12kV, just like the PGM DC-DC converters, so they too would have a relatively low bandwidth. One of the conditions for CPL behavior is that the DC-DC converter acting as the load has a much greater bandwidth than the power supply. Since this is not the case, we must account for the intermediate DC-DC converter dynamics. The duty cycle of each intermediate DC-DC converter is constant, since stabilizing control will be provided by the PGMs and HESSs.

III. Control Scheme

The control schemes of Refs. [7]-[12] rely on the ability to simplify the problem into a 2nd order single-input single-output control problem. By using a linear quadratic regulator based control scheme, the simplifying assumptions made in Refs [7]-[12] can be eliminated. DC-DC converter dynamics may be considered, not just lumped into a CPL. PGM source impedances need not conform to specific RL ratios, nor ignored. Finally, the control scheme considers the total system, not just part of it. A multiple-input control scheme allows for the combined and coordinated use of both PGMs and HESSs to improve the system transient response to step changes in load, such as from pulsed loads. A similar control scheme was used in [6] for two control sources; however, that work did not include CPLs.

A. LQR Basic Description

LQR is a popular control technique can be used on any N-dimensional system of 1st order linear differential equations [13]. Here, we focus on the time-independent or infinite-horizon variation of LQR. In state space representation, the system must be representable by (2)

$$\dot{x} = \mathrm{A}x + \mathrm{B}u \tag{2}$$

where x is an Nx1 vector of state variables and A and B are NxN positive semi-definite non-singular matrices. The solution optimizes control for a cost functional defined by (3)

$$J(t) = \frac{1}{2}\int_{t_0}^{t_f} x^T Q x + \; u^T R u \, dt \tag{3}$$

where Q is the NxN positive definite state-error cost matrix and R is the NxN positive definite input cost matrix. The control input vector u is calculated by solving the algebraic Riccati equation (4) for K and then solving for u by (5). MATLAB includes both the *care()* and *dare()* functions to solve the algebraic Riccati equation.

$$\dot{K} = 0 = -KA \; - \; A^T K \; - Q + KBR^{-1}B^T K \tag{4}$$

$$u = -R^{-1}B^T K X \tag{5}$$

The control input u will always yield a stable system (negative real part of eigenvalues). However this method has convergence issues when computation time steps are too large. Convergence issues also occur if values within the A, B, Q, or R matrices become too large or too near zero, as this can lead to matrices (or their inverses) that are singular or near singular.

B. Linearization and State-Space Representation

Since CPL impedance varies non-linearly both from loading and bus voltage, the system matrix A is variable and non-linear. To linearize the A matrix for use in LQR, we must estimate CPL load power by (6) then linearize the CPL impedance about the instantaneous operating point (7). Then, the linearized A matrix can be used by the Riccati equation (5).

$$P_{CPL_x} = Vb_x * \left(Ib_x - Cb_x \frac{d}{dt} Vb_x + Is_x\right) \quad (6)$$

$$R_{CPL} = \frac{dV}{dI} = \frac{d}{dI} V_{CPL} = \frac{d}{dI} * \frac{P_{CPL}}{I} = -\frac{P_{CPL}}{{I_{CPL}}^2} = -\frac{{Vb_x}^2}{P_{CPL}} \quad (7)$$

The system described has thirteen differential equations and only four inputs. Only the first two and last two equations in (1) provide non-zero entries in the B matrix, so the B matrix is not full rank! Since LQR requires a non-singular B matrix, we assume a full-rank B matrix and cleverly employ the R matrix to nullify the influence of zero-valued B matrix entries.

C. LQR Multi-Rate Implementation

To implement the LQR routine, the state variables are defined so that steady-state values are zero. A level shift of all of the system values which will not be zero in steady-state creates the state-variable vector 'X'.

$$\begin{aligned}
X_1 &= Ig_1 - .80 * I0 \\
X_2 &= Ig_2 - .20 * I0 \\
X_3 &= V_{bus} - V_{ref} \\
X_4 &= Iz_1 - Io1 \\
X_5 &= Iz_2 - Io2 \\
X_6 &= Vz_1 - V_{ref} - Rz_1 * Io1 \\
X_7 &= Vz_2 - V_{ref} - Rz_2 * Io2 \\
X_8 &= Vd_1 - V_{ref} - Rz_1 * Io1 \\
X_9 &= Vd_2 - V_{ref} - Rz_2 * Io2 \\
X_{10} &= Ib_1 - Iob1 \\
X_{11} &= Ib_2 - Iob2 \\
X_{12} &= Vb_1 - V_{ref1} \\
X_{13} &= Vb_2 - V_{ref2}
\end{aligned} \quad (8)$$

where:
I0 is the steady state total MVDC current.
V_{ref} is the MVDC bus reference voltage (12kV).
Io1 is the zone #1 steady state MVDC current (P_{CPL1}/V_{ref}).
Io2 is the zone #2 steady state MVDC current (P_{CPL2}/V_{ref}).
Iob1 is the zone #1 steady state LVDC current (P_{CPL1}/V_{ref1}).
Iob2 is the zone #2 steady state LVDC current (P_{CPL2}/V_{ref2}).
V_{ref1} is the zone #1 LVDC reference voltage (1kV).
V_{ref2} is the zone #2 LVDC reference voltage (6kV).

Load sharing between PGMs is enforced by choosing the steady-state PGM currents to be 80% and 20% of total load current for PGM#1 and PGM#2 respectively.

Now that we have A, B, and X, we need only develop Q and R matrices before computing control inputs. While Q and R need only be positive definite, the number of values considered in design are minimized by choosing diagonal matrices for Q and R. The Q matrix diagonals may be set according to Bryson's Rule or iteratively adjusted until results are satisfactory. Similarly the R matrix may be set using Bryson's rule or iteratively. Recall that we used a full-rank B matrix when it is in-fact sparse? Bryson's Rule would have us set the R values corresponding to null inputs to infinity, which was stated as not possible in part A of this section. In practice, null-inputs are effectively driven to negligible levels by placing the corresponding R matrix value for the input 2-3 orders of magnitude greater than the values used for non-zero inputs. In this way, we constrain the LQR algorithm to utilize only the available inputs and thus match the reality of our system.

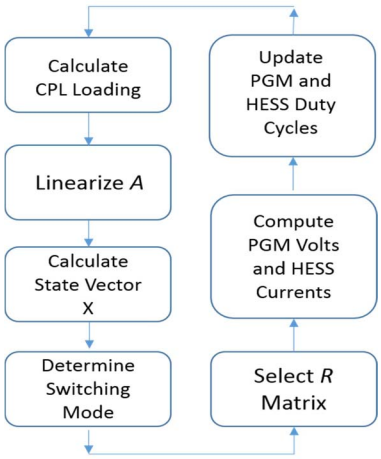

Figure 4 – Multi-rate Computation Cycle

One of the features of our system is that the HESSs operate at a higher switching frequency than the PGMs. Therefore, there will be some computation cycles where only the two HESSs are modulating current to regulate the system, as well as computation cycles where PGMs and HESSs will be simultaneously modulating. To account for this, we maintain several R matrices: one for each possible combination of inputs switching. After selecting the appropriate R matrix for the computation cycle, the Riccati equation (4) can be solved and input vector u calculated by (5).

Once u is calculated, updating the PGM voltages and HESS currents is straightforward. For cycles where PGM voltage is updated, the commanded PGM voltage is shown in (9) and (10). The commanded HESS current is shown in (11). Equations (9) and (10) include the u control term appropriate to the associated PGM as well as terms for the equilibrium voltage of the PGM.

$$E_{1_{new}} = u_{E1} + V_{ref} + Rg_1 * 0.80 * I0 \quad (9)$$

$$E_{2_{new}} = u_{E2} + V_{ref} + Rg_2 * 0.20 * I0 \quad (10)$$

$$Is_{new} = u_{Is} \quad (11)$$

Once the PGM and HESS values have been calculated, the DC-DC converter switching duty cycles for each device can be updated to produce the desired result. The full multi-rate computation cycle is illustrated in Fig. 4.

IV. Simulation and Results

The simulations presented are for the average value model of a shipboard MVDC distribution system described in Fig. 3. The MVDC main bus voltage is 12kV while the two buck zones are 1kV and 6kV respectively. It is assumed that PGM inputs may be switched at a rate of 1kHz and HESS current may be switched at a rate of 8kHz. PGM voltage switching events occur on alternating cycles such that no two PGMs are switched simultaneously. Component values are shown in Table 1. At time zero, CPL power is instantaneously stepped from 15 MW in zone #1 and 9 MW in zone #2 (total of 24 MW) to 20 MW in zone #1 and 28 MW in zone #2 (total of 48 MW). Power levels then return to their original values 10ms later. This is a step from 50% power to 100% power back to 50% power. The Q and R matrices were iteratively tuned to maintain peak voltage within 10% of reference values.

Table 1 – Component Values

Rg1	0.25 Ω	Lz1	70.5 µH	Cd1	11.1 µF
Rg2	0.30 Ω	Lz2	47.0 µH	Cd2	15.6 µF
Lg1	2.00 mH	Cz1	2.46 µF	Lb1	30.6 µH
Lg2	1.80 mH	Cz2	3.69 µF	Lb2	926 µH
Cbus	26.7 µF	Rd1	10 Ω	Cb1	75 mF
Rz1	3.30 mΩ	Rd2	10 Ω	Cb2	450 µF
Rz2	2.20 mΩ				

The simulation results demonstrate successful use of LQR-SM to control and stabilize a large transient on an MVDC bus using both PGM source voltage and HESS current as control inputs. Fig. 5a shows that PGM voltages for both PGMs are varying to stabilize the MVDC bus while Fig. 5b shows that load is being distributed between the PGMs according to their rating. PGMs #1 is supplying 80% of the current while PGMs #2 is supplying 20% of the current. The HESS currents are sourcing or sinking current to maintain zone buck voltages within the specific overshoot and undershoot limits. As the transients decay, Fig. 5c shows that HESS currents fall to zero. This demonstrates that the HESS is not used to make up the extra load current during the transient, but to suppress the voltage fluctuations on the zone buses until PGM power can supply the full load.

Fig. 6a shows that the MVDC bus voltage and the voltages at the input to each Buck converter are essentially identical. This result may indicate that cable parameters (Rzx, Lzx, Czx) are not significant and could be ignored. Fig. 6b shows the currents in the lines connecting the load zones to the MVDC bus.

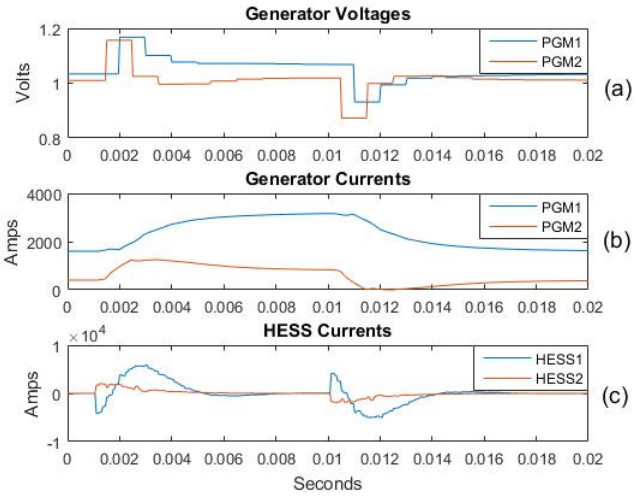

Figure 5 – PGM and HESS Inputs

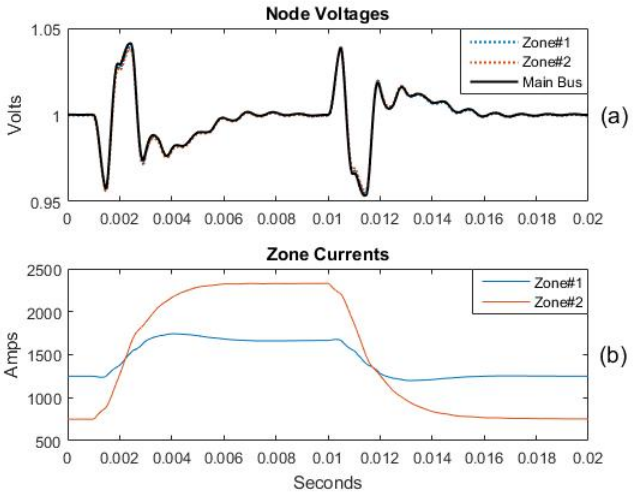

Figure 6 – MVDC Side Normalized Volts and Currents into Zone Buck Converters

Fig. 7 illustrates the same information as Fig. 6 but from the perspective of the low voltage side of the buck converters. While Fig. 6 showed that MVDC bus voltage deviated about 5% from the 12kV reference value, the zone Buck voltages deviated up to 10% from the nominal voltages of those buses. This difference is due to the additional filtering on the MVDC bus.

Overall we see that the HESS currents quickly act to provide the current demanded by the CPL while the zone Buck currents build up. By supplying current in this way, zone voltages are able to stay within the 10% voltage deviation limit desired with relatively small capacitances. The capacitors must be sized to maintain minimum voltage ripple at steady-state operation and to mitigate the severity of voltage drop during transients. For example, the HESS cannot react

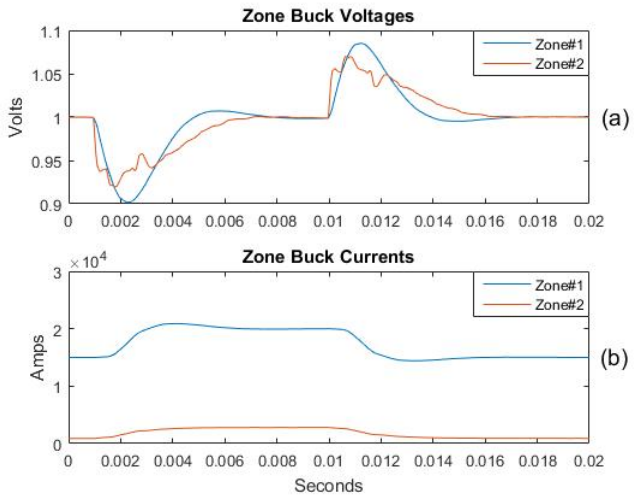

Figure 7 – Load-Side Normalized Volts and Currents from Buck Converters

sooner than one computation cycle from the time the transient is detected. The zone capacitors Cb1 and Cb2, must be sized to provide the necessary load current and maintain zone bus voltage until the HESS for that zone can supply current. The PGMs react to stabilize the voltage on the MVDC bus. Since the load currents (shown in Fig. 6b) are so smooth with very little overshoot and undershoot, the MVDC bus can be stabilized very quickly. MVDC bus stabilization time is less than 10ms.

V. Conclusion

Sparse, Multi-rate LQR is a powerful and flexible control scheme for stabilizing complex DC micro grids. Compared to other control schemes, LQR-SM has greater flexibility and ease of design. LQR-SM can be used on any system that can be modeled as a linear system. The linear system can be of any order and any number of inputs. Switching inputs be may be switched at any rate, so long as the various rates can all be related by an integer number of computation cycles. The LQR Riccati solver handles all pole-placement, so tedious transfer function derivation and feedback law design are not required.

The main disadvantage of LQR-SM is that the system is centralized. If the configuration of the distribution system changes, a new system of A, B, Q, and R matrices would have to be used to provide control. Additionally, the algebraic Riccati equation can be computationally intensive to solve, which may complicate efforts to implement the algorithm on programmable logic. Finally, determining the appropriate values for the Q and R matrices can be a time consuming iterative affair as altering the penalty for one value often leads to undesirable effects on other values.

Further, the inclusion of HESS as controllable current sources within a LQR-SM control scheme for a shipboard MVDC distribution system allows for superior bus regulation while reducing overall energy storage in the system. During transients, the HESS injects necessary current onto the LVDC buses to supply necessary load current while preventing bus voltages from drastically fluctuating. The use of the HESS in this way allows filter capacitors to be sized smaller. Since the usable energy range of a HESS is expected to be much wider than that of a bus connected capacitor, overall energy storage requirements in a system can be dramatically reduced.

VI. References

[1] John Kusean, "Naval Power Systems Technology Development Roadmap", Naval Sea Systems Command PMS 320, April 2013.

[2] Dr. Norbert Doerry, "Medium Voltage DC Power for the Future Fleet," presented as the 2015 Captain Ralph R. and Florence Peachman Lecture, Ford Presidential Library, University of Michigan Naval Architecture and Marine Engineering, Ann Arbor, Michigan, April 15, 2015.

[3] C.G. Hodge, J.O. Flower and A. Macalinden, "DC Power System Stability," *IEEE Electric Ship Technologies Symposium*, pp433-439, 2009.

[4] Lijun Gao, R. A. Dougal, and Shengyi, "Power Enhancement of an Actively Controlled Battery/Ultracapacitor Hybrid*," IEEE Transactions on Power Electronics*, Volume 20, Issue 1, pp236-243, 2005.

[5] Ahmed T. Elsayed and Osama A. Mohammed, "A Comparative Study on the Optimal Combination of Hybrid Energy Storage System for Ship Power Systems," *IEEE Electric Ship Technologies Symposium,* pp140-144, 2015.

[6] LiuJun Hou, Jing Sun and Heath Hofmann, "Interaction Analysis and Integrated Control of Hybrid Energy Storage and Generator Control System for Electric Ship Propulsion," *American Control Conference*, Chicago, IL, July 1-3, pp4988-4993, 2015.

[7] Vittorio Arcidiacono; Antonello Monti; Giorgio Sulligoi, "An Innovative Generation Control System for Improving Design and Stability of Shipboard Medium-Voltage DC Integrated Power System," *IEEE Electric Ship Technologies Symposium,* pp152 – 156, 2009.

[8] Maria Stefania Carmeli; Denis Forlani; Samuele Grillo; Roberto Pinetti; Enrico Ragaini; Enrico Tironi , "A Stabilization Method for DC Networks with Constant-Power Loads," *IEEE International Energy Conference and Exhibition (ENERGYCON),* pp617 – 622, 2012.

[9] Giorgio Sulligoi; Daniele Bosich; Lin Zhu; Marco Cupelli; Antonello Monti, "Linearizing Control of Shipboard Multi-Machine MVDC Power Systems Feeding Constant Power Loads," IEEE Energy *Conversion Congress and Exposition (ECCE),* pp691 – 697, 2012.

[10] Sulligoi, G., D. Bosich, G. Giadrossi, L. Zhu, M. Cupelli, A. Monti, "Multiconverter Medium Voltage DC Power Systems on Ships: Constant-Power Loads Instability Solution Using Linearization via State-Feedback Control," *IEEE Transactions on Smart Grid*, Vol 5, No 5, September, pp2543-2552, 2014.

[11] Marco Cupelli; Markus Mirz; Antonello Monti, "Application of Backstepping to MVDC Ship Power Systems with Constant Power Loads," *International Conference on Electrical Systems for Aircraft, Railway, Ship Propulsion and Road Vehicles (ESARS),* pp1 – 6, 2015 .

[12] Lin Zhu; Junqi Liu; Marco Cupelli; Antonello Monti, "Decentralized Linear Quadratic Gaussian Control of Multi-Generator MVDC Shipboard Power System with Constant Power Loads," *IEEE Electric Ship Technologies Symposium (ESTS),* pp308 – 313, 2013.

[13] Kirk, Donald E., "Optimal Control Theory: An introduction," Dover Publications Inc, Mineola NY, 1998.